

Article

Ongoing Conflict Makes Yemen Dark: From the Perspective of Nighttime Light

Wei Jiang ^{1,2} , Guojin He ^{1,3,4,*}, Tengfei Long ^{1,3,4,*} and Huichan Liu ^{1,3,4}

¹ Institute of Remote Sensing and Digital Earth, Chinese Academy of Sciences, Beijing 100094, China; jiangwei@radi.ac.cn (W.J.); liuhc@radi.ac.cn (H.L.)

² University of Chinese Academy of Sciences, Beijing 100049, China

³ Key Laboratory of Earth Observation Hainan Province, Sanya 572029, Hainan, China

⁴ Sanya Institute of Remote Sensing, Sanya 572029, Hainan, China

* Correspondence: hegj@radi.ac.cn (G.H.); longtf@radi.ac.cn (T.L.); Tel.: +86-010-8217-8190 (G.H.); +86-010-8217-8187(T.L.)

Received: 31 May 2017; Accepted: 1 August 2017; Published: 3 August 2017

Abstract: The Yemen conflict has caused a severe humanitarian crisis. This study aims to evaluate the Yemen crisis by making use of time series nighttime light images from the Suomi National Polar-Orbiting Partnership Visible Infrared Imaging Radiometer Suite sensor (NPP-VIIRS). We develop a process flow to correct NPP-VIIRS nighttime light from April 2012 to March 2017 by employing the Defense Meteorological Satellite Program Operational Linescan System (DMSP-OLS) stable nighttime light image. The time series analyses at national scales show that there is a sharp decline in the study period from February 2015 to June 2015 and that the total nighttime light (TNL) of Yemen decreased by 71.60% in response to the decline period. The nighttime light in all provinces also showed the same decline period, which indicates that the Saudi-led airstrikes caused widespread and severe humanitarian crisis in Yemen. Spatial pattern analysis shows that the areas of declining nighttime light are mainly concentrated in Sana'a, Dhamar, Ibb, Ta'izz, 'Adan, Shabwah and Hadramawt. According to the validation with high-resolution images, the decline in nighttime light in Western cities is caused by the damage of urban infrastructure, including airports and construction; moreover, the reason for the decline in nighttime light in eastern cities is the decrease in oil exploration. Using nighttime light remote sensing imagery, our findings suggest that war made Yemen dark and provide support for international humanitarian assistance organizations.

Keywords: Yemen crisis; nighttime light imagery; NPP/VIIRS; remote sensing; time series

1. Introduction

The Yemen crisis has lasted more than six years since it began in 2011, and it has caused severe political instability and humanitarian crisis. According to the report on Yemen released by the humanitarian response organization on 26 February 2016 [1], 21.2 million people were in need of humanitarian assistance, accounting for 81.85% of the total population of Yemen. In 2015, the Yemen humanitarian overview published by the humanitarian information unit [2] showed that over 10 million people were in need of food, water and healthcare. The Action on Armed Violence (AOAV) recorded 124 incidents in Yemen between 1 and 31 January 2015 and found a total number 5239 deaths and injuries, and this number was higher than those for Syria (4205), Iraq (3327) and Nigeria (1640). Moreover, civilians have accounted for 86% of the total number of deaths and injuries in Yemen [3].

As the conflict is extremely dangerous, it is difficult to obtain information by ground investigation [4]. Non-contact remote sensing technology has been proven to be an efficient and low-cost means to investigate armed conflicts [5]. Marx proposed a method to detect destroyed residential buildings in the Syria conflict using a time series of Landsat images, and the commission accuracy was 74%

based on ground-reference data [6]. To support humanitarian assistance, the identification and spatial extent of refugee camps can be detected with high resolution satellite imagery [7]. However, displaced camps will impact environmental conditions. A previous study showed that the rapid extension of an internally displaced persons (IDP) camp could cause the depletion of natural resources in Sudan [8]. Moreover, the normalized difference vegetation index (NDVI) was employed to measure eco-scarcity during the war [9], and some studies further investigated the impact of conflict on forest cover change [10,11] and forest degradation [12].

Generally, war will destroy urban public infrastructure, such as airports, roads and houses, and will result in dramatic changes in human activity. Among the various remote sensing platforms, nighttime light remote sensing can provide unique spatial observations linked with human activity [13]. Consequently, nighttime light remote sensing has been used in various fields, such as social and economic parameters estimation [14–16], urban monitoring [17–21], gas flaring detection [22,23], environment and health effects [24–27], and humanitarian crises [28–30]. In addition, nighttime light remote sensing has been proven to be an efficient tool in detecting global armed conflicts [28]. Recent studies have investigated the Syrian crisis [30,31], the Iran crisis [4], and the war between Russia and Georgia [32] by using time series nighttime light remote sensing images. Coscieme et al. developed a regional disparity index based on nighttime light images, and this index could help to forecast where conflicts are likely to break out [33].

At present, there are two types of commonly used nighttime remote sensing data: the Defense Meteorological Satellite Program Operational Linescan System (DMSP-OLS) and the Suomi National Polar-Orbiting Partnership Visible Infrared Imaging Radiometer Suite (NPP-VIIRS) [34]. DMSP-OLS is the longest running nighttime light satellite with yearly products from 1992–2013; however, the weaknesses of DMSP-OLS data are the coarse spatial resolution, low radiometric resolution and lack of on-board radiometric calibration [35,36]. Fortunately, the new generation of NPP-VIIRS nighttime light data was released by the National Oceanic and Atmosphere Administration (NOAA), and VIIRS recorded its first image on November 2011, with data available from 2012. The performance improvements, including higher spatial resolution, radiometric detection capacity and no saturation in urban areas, indicate that it has more potential for various applications [37,38]. Moreover, the NPP-VIIRS nighttime light data is a monthly product, and it can be used to demonstrate rapid human activity change patterns [4].

In previous studies, the DMSP-OLS was mainly applied as a nighttime light data source to evaluate wars [30,32]. A recent study documented the application potential of NPP-VIIRS nighttime light data in wars [4]. In this study, the primary objective is to evaluate the Yemen crisis using time series NPP-VIIRS nighttime light images from April 2012 to March 2017. The NPP-VIIRS images need to be preprocessed to remove background noise and reduce gas flare effects. Then, the trend method and nighttime light indexes are employed to evaluate the patterns of spatial-temporal change in nighttime light at different administrative levels. In addition, reasons for nighttime light change are identified using high resolution satellite remote sensing images. This study provides a new perspective for understanding the ongoing Yemen crisis, and it has potential applications for Yemen humanitarian assistance.

2. Materials and Methods

2.1. Study Area

Yemen is located in Western Asia and is bordered by the Arabian Sea, the Red Sea and Saudi Arabia, occupying 527,970 km², as shown in Figure 1. The Yemen crisis began in 2011 and can be divided into four stages, which include the revolution (2011–2012), the transitional period (2012–2014), the Houthi rebellion (2014–2015) and the war in Yemen (2015–present) [39,40]. Figure 2 shows the timeline of key events during the Yemen crisis. The latter two stages, including the Houthi rebellion and the war in Yemen, attracted widespread concern from the international community due to the severe

humanitarian crisis. Sa’dah was a Houthis-controlled city before 2014, and Sana’a is the capital of Yemen, which is controlled by the government. When Sana’a was captured by the Houthis in September 2014, President Hadi arrived in ‘Adan, and ‘Adan became a provisional capital. After the Houthis attacked ‘Adan, Hadi left for Saudi Arabia, and then, the Saudi-led airstrikes began on 26 March 2015.

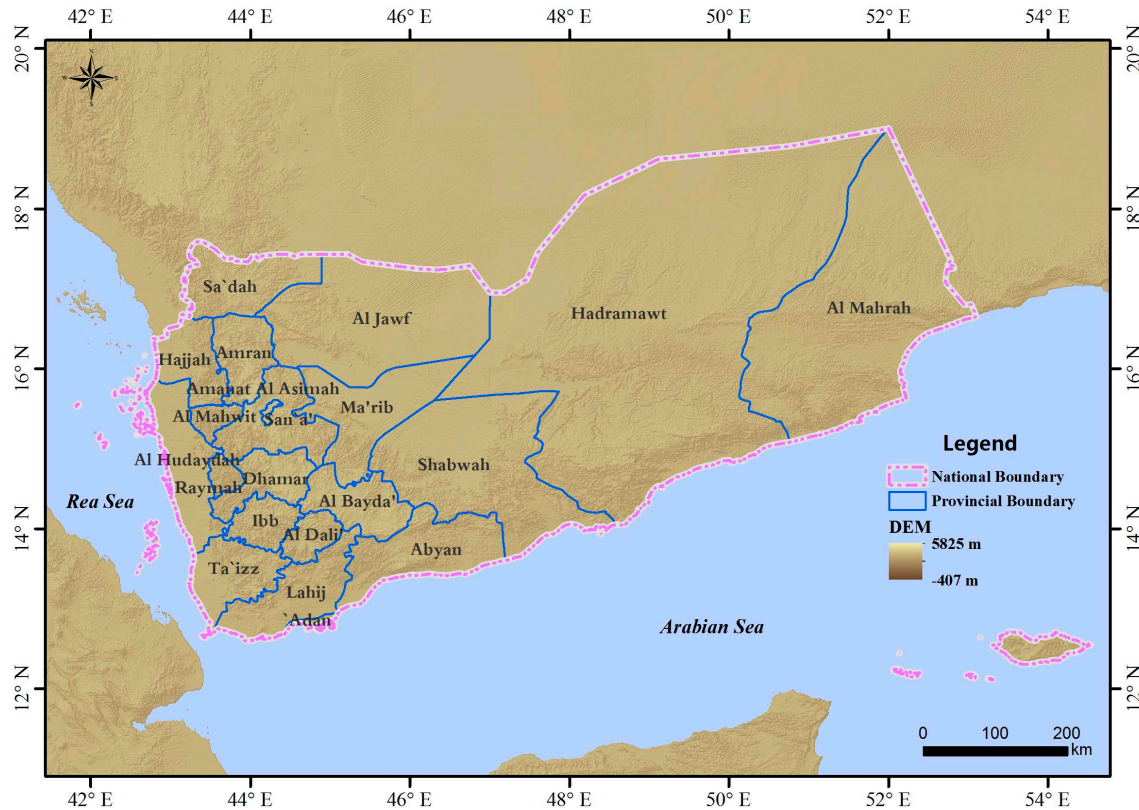


Figure 1. An administrative map of Yemen.



Figure 2. A timeline of the Yemen crisis.

2.2. Data Source

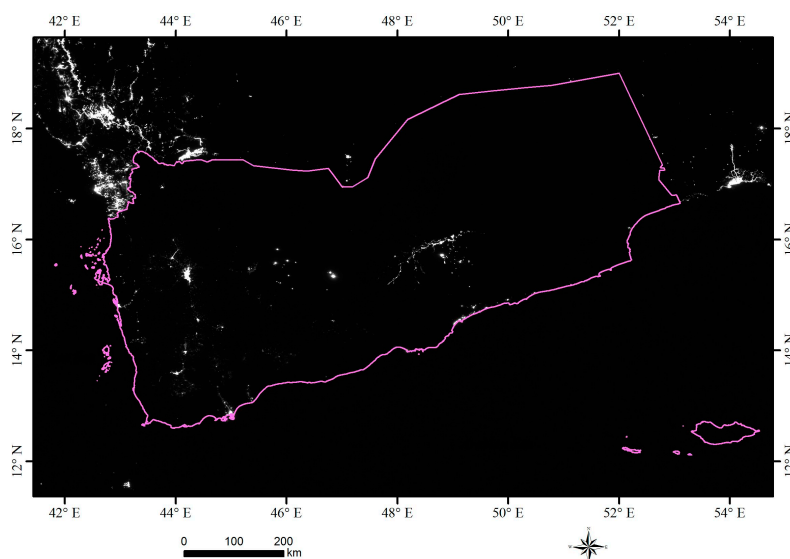
2.2.1. Nighttime Light Imagery

In this study, the NPP-VIIRS and DMSP-OLS are selected as the observational data to evaluate the Yemen crisis. The parameters of NPP-VIIRS and DMSP-OLS are presented in Table 1. Compared with DMSP-OLS nighttime light imagery, the capability of NPP-VIIRS has been improved significantly in terms of spatial resolution, radiation resolution, on-board calibration and temporal resolution. The NPP-VIIRS nighttime light product eliminated clouds, stray light, lightning, moonlight, and other factors; however, the Aurora, fire point, vessel and luminous change information were not removed. Human activity changes in conflict crisis areas are more rapid than in peaceful areas; thus, we selected the higher spatial and temporal resolution NPP-VIIRS nighttime light images to investigate the Yemen crisis. To remove the background noise, the DMSP-OLS was employed to preprocess the NPP-VIIRS.

Table 1. The parameters of NPP-VIIRS and DMSP-OLS

Parameters	NPP-VIIRS	DMSP-OLS
Operator	National Aeronautics and Space Administration (NASA) and National Oceanic and Atmospheric Administration (NOAA)	Department of Defense, United States
Orbit	Polar orbit satellite	Polar orbit satellite
Overpass time	13:30 and 1:30	8:30–9:30 and 20:30–21:30
Width	3040 km	3000 km
Temporal resolution	12 h	12 h
Spatial resolution	742 m	2.7 km
Wavelength range	0.5–0.9 μm	0.4–1.1 μm
Radiation resolution	14 bit	6 bit
Unit	$\text{W}\cdot\text{cm}^{-2}\cdot\text{sr}^{-1}\cdot\mu\text{m}^{-1}$	Relative (0–63 scale)
On-board calibration	Yes	No
Pixel saturated	No saturated	Saturated
Available product	December 2011–now	1992–2013
Product cycle	Month	Year

The Suomi National Polar-orbiting Partnership (S-NPP) satellite was launched in October 2011, carrying 5 sensors. VIIRS is one of the key sensors, with 22 bands, and nighttime light is observed by the Day/Night band. The released NPP-VIIRS nighttime light product is in version 1 and can be freely downloaded from the National Centers for Environmental Information (NCEI) in NOAA [41]. The global product of NPP-VIIRS nighttime light is divided into six parts, and the product used here is the monthly average radiation brightness synthesis. According to the Yemen crisis timeline, we chose NPP-VIIRS nighttime light images from April 2012 to March 2017. Images from January 2014 and December 2015 are shown in Figure 3.

**(a)****Figure 3.** Cont.

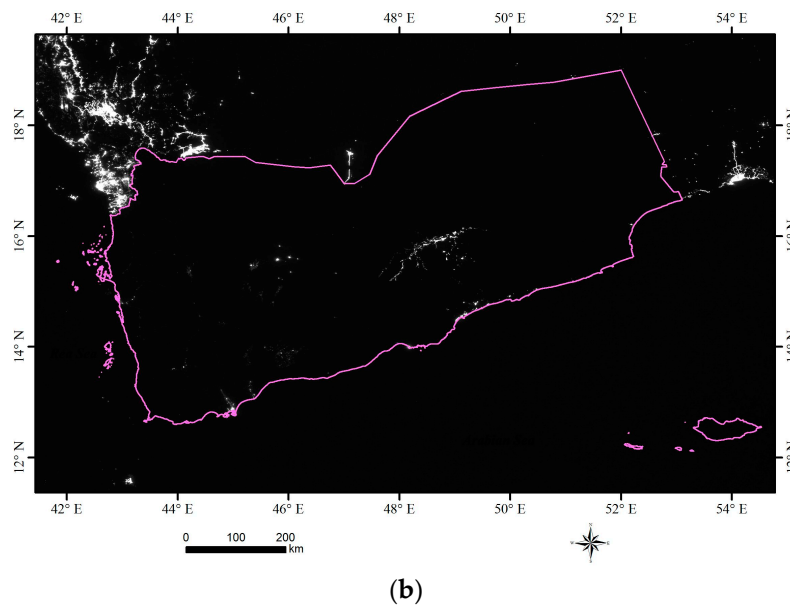


Figure 3. NPP-VIIRS nighttime light images of Yemen from (a) January 2014 and (b) December 2015.

DMSP/OLS data are the longest time series nighttime light imagery, available from 1992 to 2013. The version 4 dataset contains three products: the frequency of the cloud-free product, the average light product, and the stable nighttime light product. These products can be freely downloaded from the NCEI in NOAA [42]. These products were provided at 30 arc second grids, spanning -180 to 180 degrees longitude and -65 to 75 degrees latitude. Because NPP-VIIRS images were chosen from 2012 to 2017, we selected the DMSP-OLS stable nighttime light product for 2013 (Figure 4), which is close to the acquisition year of NPP-VIIRS. This product contains stable nighttime light from cities, towns, gas flares and ephemera, while fires have been removed. In addition, the background noise has been detected and replaced with values of zero. Data values range from 0 (background) to 63 (brightest), and the digital numbers (DNs) are saturated at the core of urban areas.

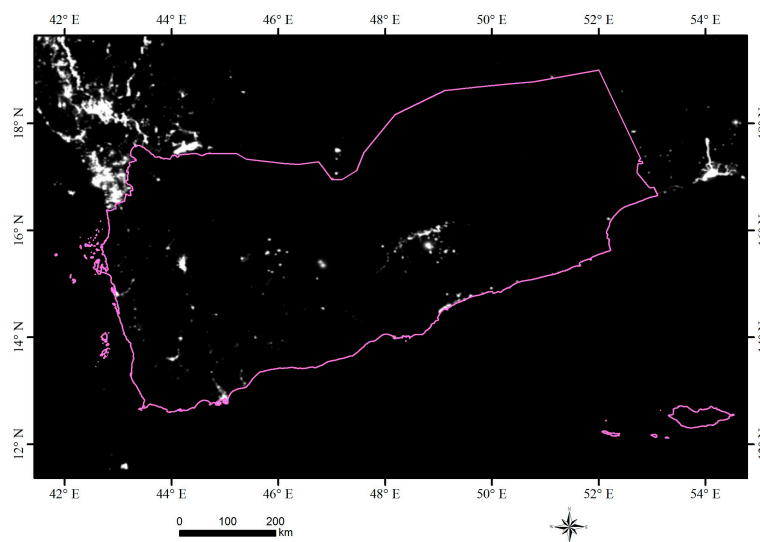


Figure 4. DMSP-OLS nighttime light images of Yemen from 2013.

2.2.2. Auxiliary Data

To investigate the nighttime light change patterns within different administrative regions, the national and provincial boundaries of Yemen were acquired from the Global Administrative Areas website [43]. The coordinate reference system of the boundary file is longitude/latitude in the WGS84 datum. In addition, high-resolution images from Google Earth were selected to identify the causes of nighttime light change.

2.3. Nighttime Light Imagery Processing

The background noise and gas flaring of NPP-VIIRS will create evaluation uncertainty when using the NPP-VIIRS nighttime light imagery [4]. To objectively evaluate the Northern Iraq humanitarian crisis, Li et al. proposed a method to generate a mask for the city lights of NPP-VIIRS by employing a global 500 m urban extent map from 2001 [4]. However, due to the scattering characteristic of nighttime light, the extent of nighttime light is often larger than that of urban areas. Considering the uncertainty of NPP-VIIRS background noise in estimating socioeconomic parameters, previous studies [34,35] proposed the assumption that lit areas were the same between two types of nighttime light images and generated lit area masks with the positive value pixels of DMSP-OLS for removing the background noise. In this study, we focused on the urban area nighttime light and an efficient method proposed by Zhao and Samson [44] by setting 10 as the DN threshold to extract city areas. Thus, the city mask in this paper is generated by the following formula:

$$DN_{mask} = \begin{cases} 0 & DN_{OLS} < 10 \\ 1 & DN_{OLS} \geq 10 \end{cases} \quad (1)$$

where DN_{OLS} represents the DN value of the DMSP-OLS nighttime light image and DN_{mask} represents the DN value of the urban area mask.

Because Yemen is an oil-rich country, the DN values of gas flares observed in nighttime light images are larger than those of urban areas. Previous studies [45,46] proposed a VIIRS night-fire algorithm to detect gas flares, and the daily detection products of gas flares are available [47]. According to a previous study [48], the radiance nighttime light across fossil fuel burning emissions was greater than $90 \times 10^{-9} \text{ W}\cdot\text{cm}^{-9}\cdot\text{sr}^{-1}$. To demonstrate the nighttime light change characteristics, $300 \times 10^{-9} \text{ W}\cdot\text{cm}^{-9}\cdot\text{sr}^{-1}$ was selected as the threshold to reduce gas flare effects. Therefore, we proposed a workflow (Figure 5) to process the NPP-VIIRS nighttime light images.

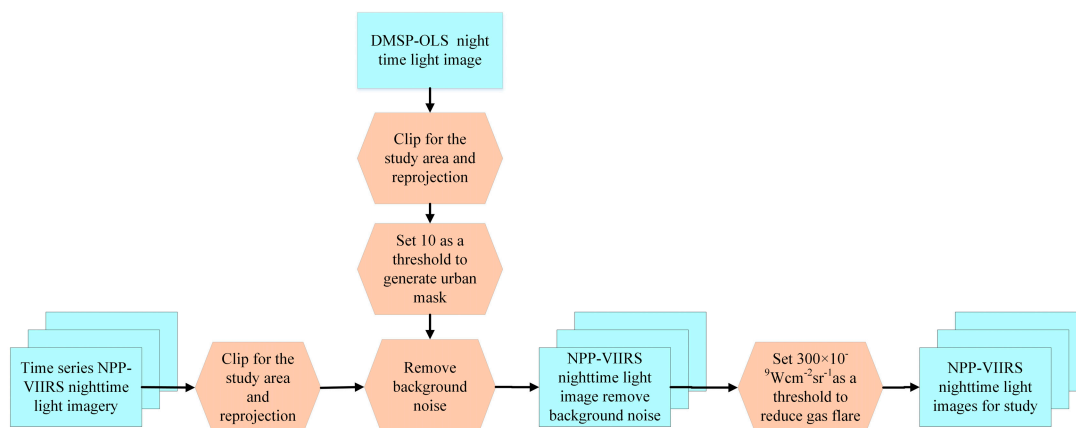


Figure 5. Processing flow of the NPP-VIIRS nighttime light images.

In the workflow, the two types of nighttime light images (NPP-VIIRS and DMSP-OLS) need to be first clipped and re-projected. According to the threshold method, a city mask based on the

DMSP-OLS nighttime light image in 2013 was generated (Figure 6). The city mask was applied to multiple NPP-VIIRS nighttime light images to remove background noise. Then, gas flares were further reduced by the threshold method. The local areas of the original image and the corrected image are shown in Figure 7. It can be seen that some background noise in the original image was removed, and the contrast of the corrected image was higher than that of the original image.

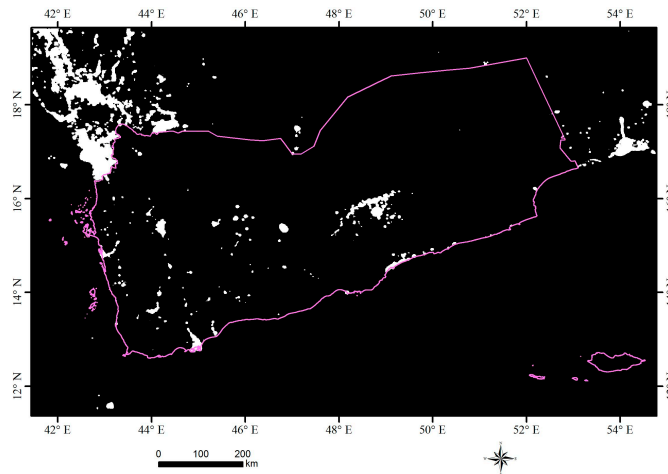


Figure 6. The Yemen city mask based on DMSP-OLS nighttime light images.

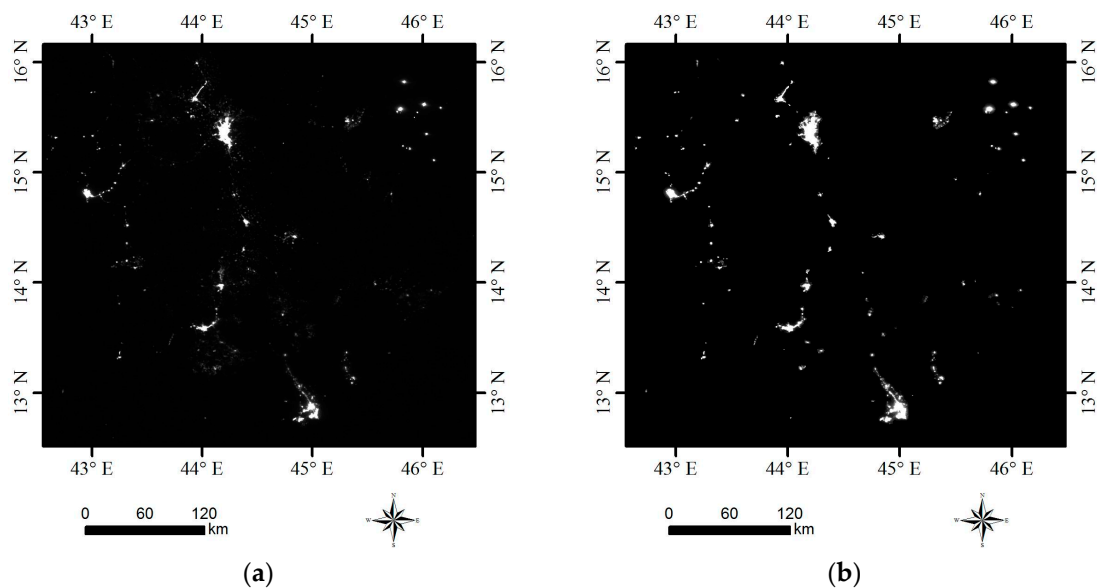


Figure 7. Nighttime light images before and after correction: (a) original image and (b) corrected image.

2.4. Method

2.4.1. Theil-Sen Median Trend Method

To reveal the change characteristics of time series nighttime light in Yemen, the Theil-Sen Median trend method was adopted. The Theil-Sen Median is a robust trend analysis method with non-parametric statistics [49] and is a particularly effective tool for estimating the trends in small series [49,50]. The Theil-Sen Median has been widely used to test the trend of time series remote

sensing images [51–53], especially in long time series of vegetation variation analysis [49,50,52]. The formula is as follows:

$$S_{VIIRS} = \text{Median}\left(\frac{DN_j - DN_i}{j - i}\right) \quad 1 \leq i \leq j \leq 24 \quad (2)$$

where S_{VIIRS} refers to the median slope between $n(n-1)/2$ pairs of time series NPP-VIIRS nighttime light images; and DN_j and DN_i , represent the DN values of the pixels in month j and month i , respectively. In the case of $S_{VIIRS} > 0$, it represents an increase trend of nighttime light; in case of $S_{VIIRS} < 0$, it represents a decline trend of nighttime light; $S_{VIIRS} = 0$ means a stable trend of nighttime light.

2.4.2. Nighttime Light Indexes

Total nighttime light (TNL) represents the total level of nighttime light, and previous studies have confirmed that it relates strongly to GDP [48], population [54] and other socio-economic parameters [16]. In this study, we employed TNL as the indicator to analyze nighttime light change patterns at different administrative scales, and the formula is as follows:

$$TNL = \sum_{i=0}^{300} C_i DN_i \quad (3)$$

where DN_i is i th the DN value and C_i is the number of pixels corresponding to each DN value.

To show the spatial change of nighttime light during the two periods, a nighttime light difference index (NLDI) was developed in this paper. The index is used to demonstrate change patterns of nighttime light by calculating the difference between the two temporal images. The equation is as follows:

$$NLDI = \varphi^{t1} - \varphi^{t2} \quad (4)$$

where φ^{t1} and φ^{t2} denote the image at t_1 and t_2 periods, respectively.

During the conflict period, the nighttime light usually fluctuates. Therefore, we adopted the nighttime light change rate index (NLCRI) proposed by Li et al. [55] to quantitatively evaluate nighttime light changes, and the equation is as follows:

$$NLCRI = \frac{TNL_m - TNL_n}{TNL_n} \times 100\% \quad (5)$$

where TNL_m and TNL_n denote the total nighttime light of the m period and n period, respectively.

3. Results

3.1. Time Series Analysis

TNL can be used to demonstrate the level of nighttime light for countries and provincial regions, and it relates to human activity [27]. The TNL of Yemen from April 2012 to March 2017 was calculated for each month (Figure 8). From the TNL change at a national scale, there is a seasonal change from March to June for each year that may relate to surface reflectance and atmospheric conditions [56]. Compared with the nighttime change in each year, a sharp decline period can be found from February 2015 to June 2015 and it lasted for 4 months. The TNL showed some fluctuation in other periods. Combined with the timeline of the Yemen crisis, the decline period related to Saudi-led airstrikes. Moreover, the NLCRI was calculated based on TNL (Figure 8) to quantitatively assess nighttime light change. TNL lost 71.60% corresponded to the decline period. Among the 4 months, the TNL from March 2015 to April 2015 dropped the most (49.18%), followed by the months from April 2015 to June 2015 at 31.16%.

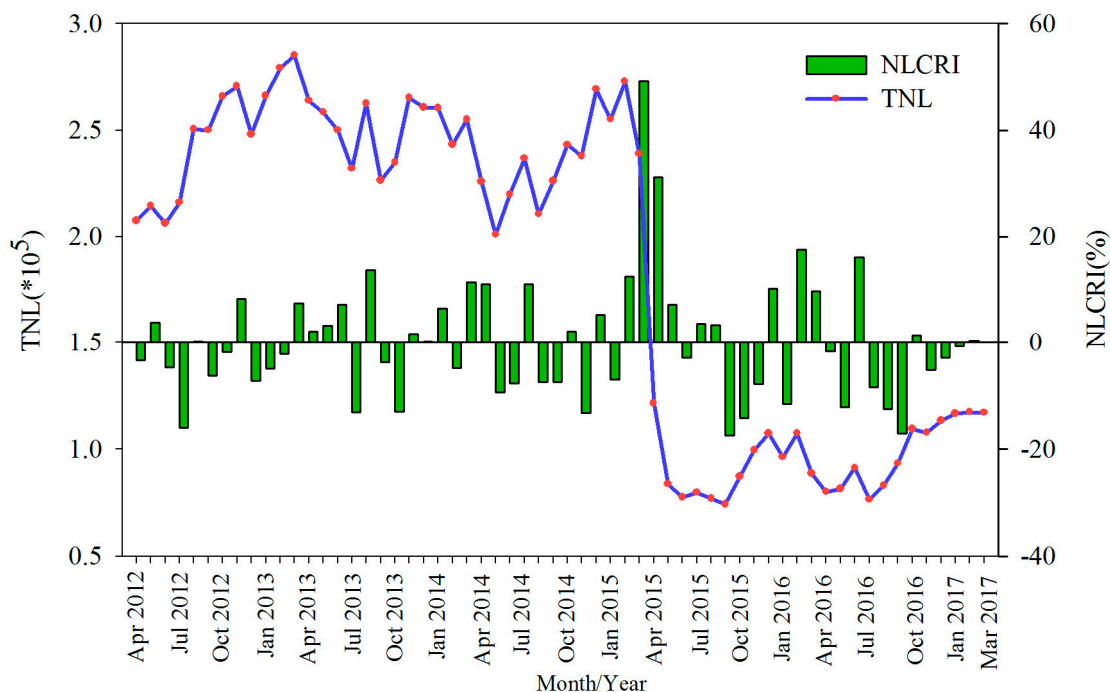


Figure 8. TNL of Yemen from April 2012 to March 2017 at a national scale.

The TNL of each province was calculated from April 2012 to March 2017 (Figure 9). All provinces exhibited sharp decline in TNL from February 2015 to June 2015. This result is consistent with the change pattern of TNL at the national scale. There was no nighttime light detected by the VIIRS sensor in Raymah, and the TNL of Raymah was zero.

To explore the changing characteristics of nighttime light at a provincial scale during the decline period, the NLCRIs were calculated for each province (Figure 10). The decline of nighttime light in Amran, Amanat Al Asimah, Al Mahwit, San'a', Dhamar, Ibb, Al Dali' and Lahij was greater than that of other provinces. Among the all provinces, the fastest decline of nighttime light occurred in Dhamar (92.41%), followed by Ibb (91.12%). This result indicates that the impact of the conflict during the decline period was severe and wide and the highly impacted areas were mainly concentrated in west region. In addition, as Sa'dah was captured by Houthis before 2014, its NLCRI declined by 7.44% from March 2014 to May in 2014; however, the provisional capital of Sa'dah was attacked by the Saudi-led airstrikes during decline period in 2015, and the decline of nighttime light was 61.94%.

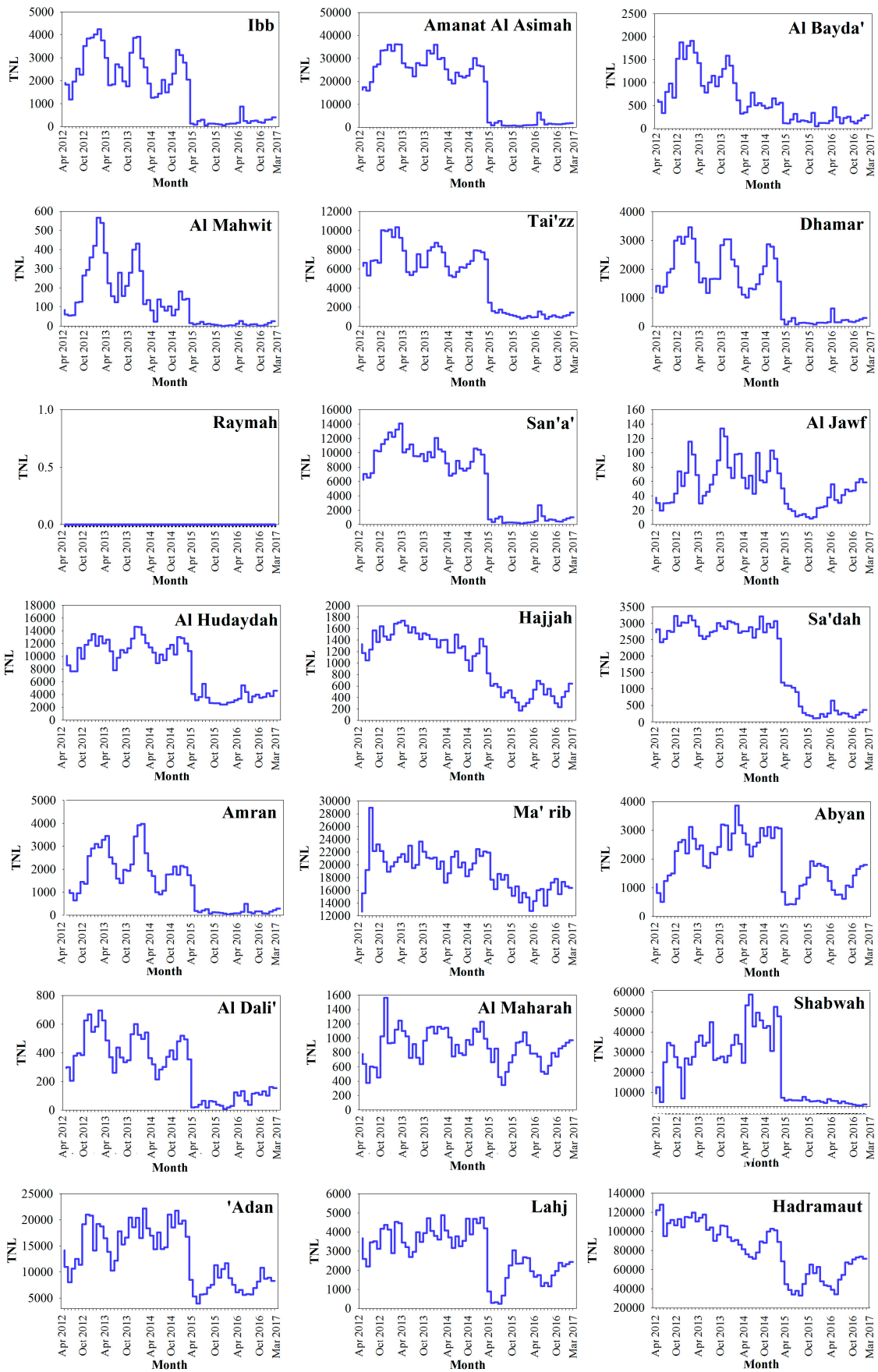


Figure 9. TNL of Yemen from April 2012 to March 2017 at the provincial scale.

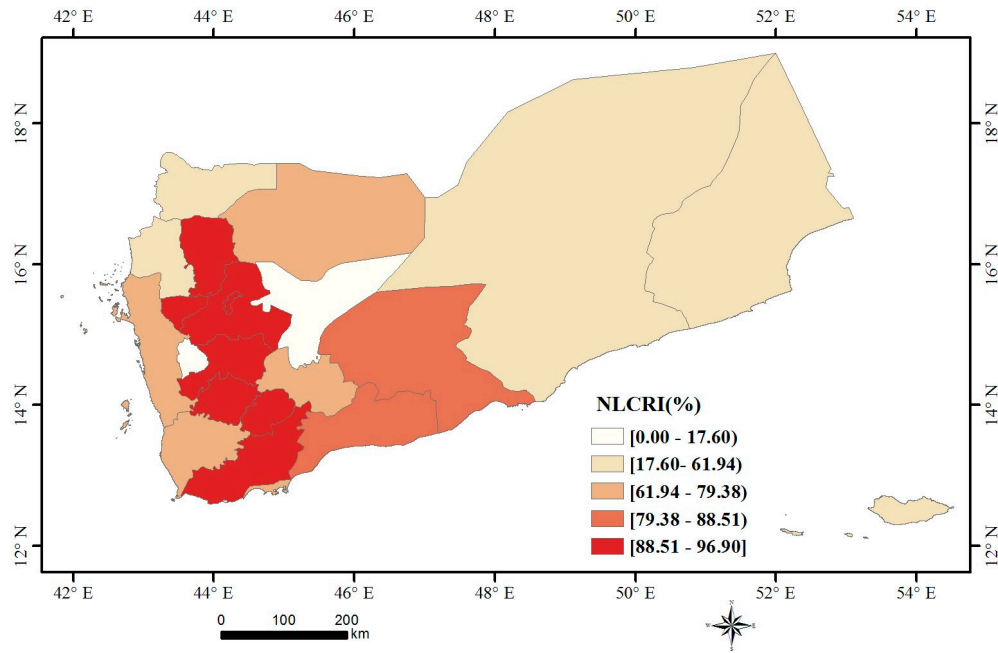


Figure 10. Nighttime light change rate index (NLCRI) for Yemen from February 2015 to June 2015.

3.2. Spatial Pattern Analysis

The Theil-Sen Median trend method was employed to understand the spatial pattern changes of nighttime light in Yemen from April 2012 to March 2017, as shown in Figure 11. The figure shows that the areas of nighttime light decline were mainly concentrated in the capital cities of Sana’a, ‘Adan, Shabwah and Hadramawt. Moreover, the nighttime light of the capital cities of Sa’dah, Amran, Dhamar, Ibb and Ta’izz also show a decreasing trend. In addition, the nighttime light trend of the southwest area of Saudi Arabia, which is close to northern Yemen, shows a stable trend. This result provides the evidence that the declines in Yemen are real and not just a sensor calibration issue.

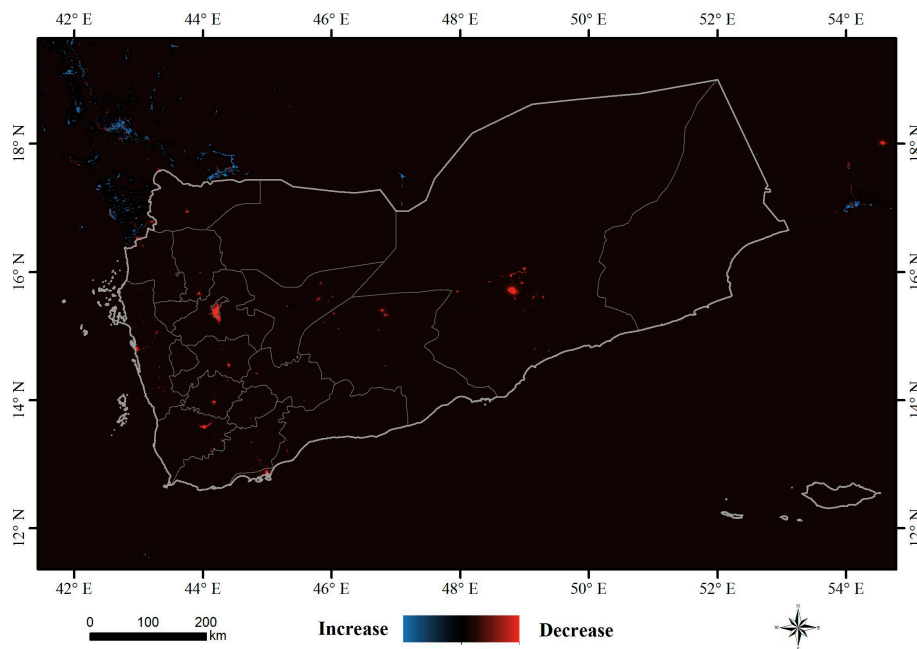


Figure 11. Change in nighttime light from April 2012 to March 2017 in Yemen

To investigate the spatial pattern changes in nighttime light in Yemen during the conflict crisis period (February 2015 to June 2015), the NLDI method was applied by using the corresponding images. Figure 12 is the spatial pattern change of nighttime light images from February 2015 to June 2015. The change trend is relatively consistent with the result of the Theil-Sen Median trend, and those areas are mainly located in Sana'a, Dhamar, Ibb, Ta'izz, 'Adan, Shabwah and Hadramawt.

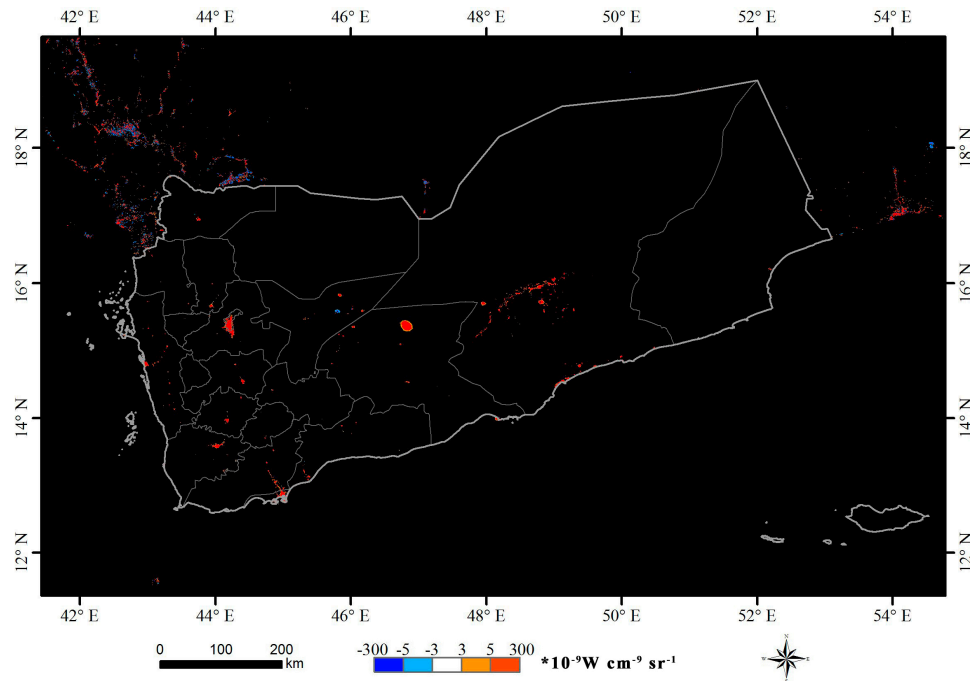


Figure 12. The spatial patterns of change in nighttime light during conflict period.

To investigate the causes of nighttime light change during the crisis period in Yemen, high-resolution images from Google Earth were acquired for validation in key cities. Figure 13 represents the destruction of infrastructure in Sana'a, Sa'dah and 'Adan from 2014 to 2016. From Figure 13(a1,a2,e1,e2,j1,j2), it can be observed that airports were the fundamental infrastructure destroyed, and the main destruction targets in airports were aircraft and airport runways. The other sites represent the destruction of construction. From the view of the fragmentation of construction after destruction, these destructions were likely caused by missiles. In the damaged construction, mosques were also one of the damaged targets.

Generally, the nighttime light declines were mainly caused by the destruction of urban facilities during the war. However, according to the validation result (Figure 14), the main factor of nighttime light decline in Shabwah and Hadramawt was oil exploration. This is because nighttime light remote sensing technology can capture gas flaring during the process of oil exploration. When oil exploration decreases or stops, the gas flaring will correspondingly decrease or stop; thus, the pattern of nighttime light in oil exploration areas shows a declining trend.



Figure 13. Validation of the infrastructure destruction in Sana'a, Sa'dah and 'Adan: (a1,a2,b1,b2,c1,c2,d1,d2) represent infrastructure destruction before and after war in Sana'a; (e1,e2,f1,f2,g1,g2,h1,h2) represent infrastructure destruction before and after war in Sa'dah; and (i1,i2,j1,j2) represent infrastructure destruction before and after war in 'Adan.

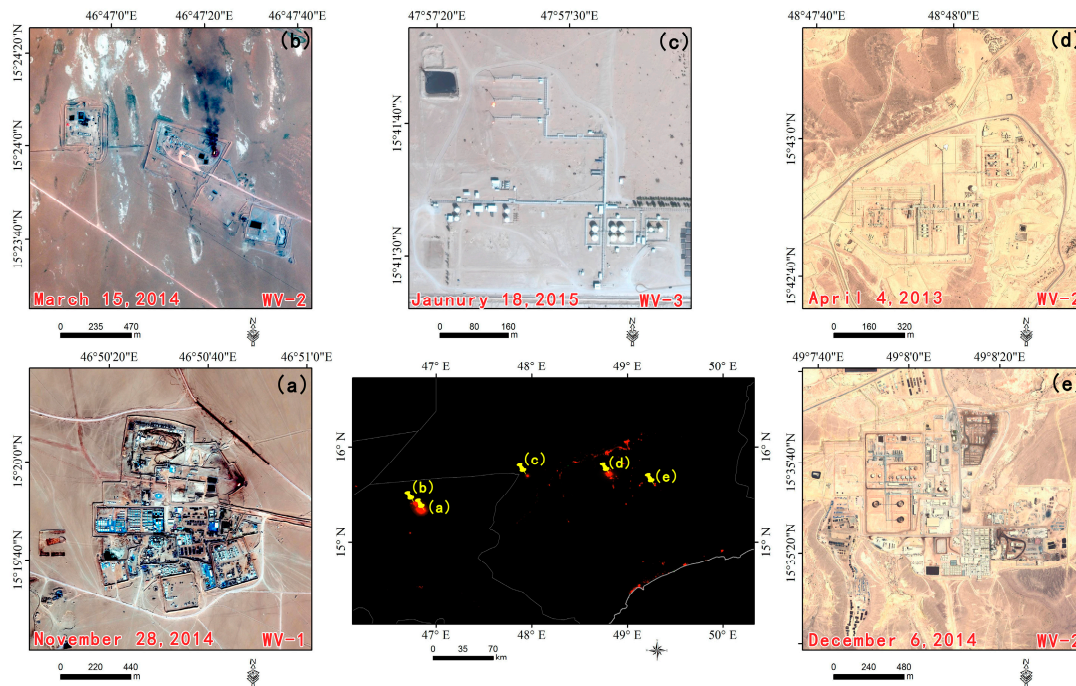


Figure 14. Validation of the oil exploration in Shabwah and Hadramawt: (a,b) represent oil exploration areas in Shabwah, and (c–e) represent oil exploration areas in Hadramawt.

4. Discussion

Up to 31 December 2016, the Yemen crisis has caused nearly 48,000 casualties (including nearly 7500 deaths) and attracted the attention and humanitarian relief of the international community [57]. Despite some humanitarian reports related to the Yemen crisis released by the Office for the Coordination of Humanitarian Affairs (OCHA) [57], the perspective from nighttime light remote sensing to evaluate the Yemen crisis is still lacking. Commonly, nighttime light is highly related to human socio-economic activities, and the war will inevitably slow down or stop socio-economic development [30] and even result in an economic recession. Therefore, nighttime light remote sensing technology is a useful tool to evaluate the war with the advantages of safety, convenience and low cost [28]. In this study, the new generation of nighttime light images from NPP-VIIRS in Yemen was obtained from April 2012 to March 2017. We develop a process flow to eliminate background noise and reduce gas flare using the DMSP-OLS stable nighttime light images. Then, a trend method and nighttime index were proposed to analyze time series changes and spatial patterns of changes in nighttime light. Finally, high-resolution images from Google Earth were selected to validate the causes of nighttime light change.

From time series analysis, a sharp decline period of nighttime light at the national scale was found, and the nighttime light lost 71.60% from February 2015 to June 2015. The TNL in all provinces also showed decline responded to the period. These results showed that the crisis was widespread and severe. This is because the crisis was Saudi-led airstrikes against the Houthis and fighting escalated nationwide [58], and this attack bombed civilian infrastructure, such as factories, bridges and power stations [59].

From the spatial pattern of changes in nighttime light in Yemen, the areas of decline were mainly located in Sana'a, Dhamar, Ibb, Ta'izz, 'Adan, Shabwah and Hadramawt, and the nighttime light of other capital cities also showed a declining trend. Based on the results of validation with high resolution images, the nighttime light decline in western cities (Sana'a, Sa'dah and 'Adan) was mainly due to the damage of urban infrastructure, including airports [60] and construction [61]; however, the main reason for the nighttime light decline in eastern cities (Shabwah and Hadramawt) was that oil exploration

decreased or stopped. According to the statistical data of trading economics [62], the crude oil production of Yemen began to sharply drop in July 2015 and continued to decrease for more than one year. This evidence indicates that the decrease in oil exploration, which was affected by the conflict, is the main cause for the nighttime light decline in Shabwah and Hadramawt. This finding can back up the previous understanding [63] that nighttime light decline is due to the destruction of urban human settlement.

In fact, there are two other important factors related to nighttime light decline that cannot be ignored. The first factor is the nighttime curfew policy. To avoid night attacks during the conflict, the government declared nighttime curfews in Sana'a [64] and Aden [65], and the implementation of this policy directly led to a decline in nighttime light. Another factor is electrical blackouts [66]. Because electricity infrastructure is often damaged and power supply is insufficient during wars, electrical blackouts are likely to occur. This condition can also result in the decline of nighttime light.

5. Conclusions

The Yemen war has been a severe humanitarian crisis since 2011. Traditional ground investigation is dangerous and expensive. Therefore, this study provides an evaluation of the Yemen crisis by making use of a time series of the new generation of NPP-VIIRS nighttime light images. The corrected NPP-VIIRS nighttime light images were generated using the developed flow with the DMSP-OLS stable nighttime light images. Then, the Theil-Sen Median trend method and nighttime light index were employed to explore the time series patterns and spatial change patterns, respectively. The conclusions are summarized as follows:

- (1) At the national scale, nighttime light showed a sharp decline from February 2015 to June 2015, and TNL lost 71.60%. The nighttime light in all provinces also showed the decline period. These findings reflect that the Saudi-led airstrikes caused widespread and severe humanitarian crisis in Yemen.
- (2) From spatial pattern analysis, the areas of decline were found to be mainly located in Sana'a, Dhamar, Ibb, Ta'izz, 'Adan, Shabwah and Hadramawt. The validation results show that the nighttime light declines in western cities and eastern cities are due to the damage of urban infrastructure and decreased oil exploration, respectively. In addition, a nighttime curfew policy and electrical blackouts are also key factors in the decline of nighttime light in Yemen.

This study provides strong evidence for understanding how severe the Yemen humanitarian crisis is and confirms that the ongoing conflict Saudi-led airstrikes has made Yemen dark. These conclusions will be helpful for Yemen humanitarian assistance. In addition, the efficient and convenient evaluation method proposed in this study can also be used to investigate other conflicts. In future studies, the background noise of NPP-VIIRS nighttime light images needs to be accurately separated from human-induced light. Moreover, the NPP-VIIRS stable nighttime light product needs to be generated to remove occasional lights. Thus, the stable nighttime light products of NPP-VIIRS and DMSP-OLS can be integrated to assess the effects of conflict on human activities.

Acknowledgments: This research was financially supported by the National Key Research and Development Program of China—Rapid production method of large scale global change products (2016YFA0600302), and the Hainan Provincial Department of Science and Technology under Grant Nos. ZDKJ2016021 and ZDKJ2016015. The authors thank editors and three anonymous reviewers for their valuable comments to improve our manuscript.

Author Contributions: Guojin He and Wei Jiang conceived and designed the experiments; Wei Jiang performed the experiments; Wei Jiang, Tengfei Long and Huichan Liu analyzed the data; Wei Jiang wrote the paper; and all authors edited the paper.

Conflicts of Interest: The authors declare no conflict of interest.

References

1. Yemen Humanitarian Response. Available online: <https://www.humanitarianresponse.info/en/home> (accessed on 29 August 2016).
2. Humanitarian Information Unit. Available online: <https://hiu.state.gov/> (accessed on 29 August 2016).
3. State of Crisis: Explosive Weapons in Yemen. Available online: <https://aoav.org.uk/wp-content/uploads/2015/09/State-of-Crisis-A4.pdf> (accessed on 29 August 2016).
4. Li, X.; Zhang, R.; Huang, C.Q.; Li, D.R. Detecting 2014 northern Iraq insurgency using nighttime light imagery. *Int. J. Remote Sens.* **2015**, *36*, 3446–3458. [[CrossRef](#)]
5. Witmer, F.D.W. Remote sensing of violent conflict: Eyes from above. *Int. J. Remote Sens.* **2015**, *36*, 2326–2352. [[CrossRef](#)]
6. Marx, A.J. Detecting urban destruction in Syria: A landsat-based approach. *Remote Sens. Appl. Soc. Environ.* **2016**, *4*, 30–36. [[CrossRef](#)]
7. Giada, S.; De Groeve, T.; Ehrlich, D.; Soille, P. Information extraction from very high resolution satellite imagery over Lukole refugee camp, Tanzania. *Int. J. Remote Sens.* **2003**, *24*, 4251–4266. [[CrossRef](#)]
8. Hagenlocher, M.; Lang, S.; Tiede, D. Integrated assessment of the environmental impact of an IDP Camp in Sudan based on very high resolution multi-temporal satellite imagery. *Remote Sens. Environ.* **2012**, *126*, 27–38. [[CrossRef](#)]
9. Brown, I.A. Assessing eco-scarcity as a cause of the outbreak of conflict in Darfur: A remote sensing approach. *Int. J. Remote Sens.* **2010**, *31*, 2513–2520. [[CrossRef](#)]
10. Stevens, K.; Campbell, L.; Urquhart, G.; Kramer, D.; Qi, J.G. Examining complexities of forest cover change during armed conflict on Nicaragua’s Atlantic Coast. *Biodivers. Conserv.* **2011**, *20*, 2597–2613. [[CrossRef](#)]
11. Gorsevski, V.; Kasischke, E.; Dempewolf, J.; Loboda, T.; Grossmann, F. Analysis of the impacts of armed conflict on the eastern afro-montane forest region on the South Sudan—Uganda border using multitemporal landsat imagery. *Remote Sens. Environ.* **2012**, *118*, 10–20. [[CrossRef](#)]
12. Nackoney, J.; Molinario, G.; Potapov, P.; Turubanova, S.; Hansen, M.C.; Furuichi, T. Impacts of civil conflict on primary forest habitat in Northern Democratic Republic of the Congo, 1990–2010. *Biol. Conserv.* **2014**, *170*, 321–328. [[CrossRef](#)]
13. Elvidge, C.D.; Cinzano, P.; Pettit, D.R.; Arvesen, J.; Sutton, P.; Small, C.; Nemani, R.; Longcore, T.; Rich, C.; Safran, J.; et al. The nightsat mission concept. *Int. J. Remote Sens.* **2007**, *28*, 2645–2670. [[CrossRef](#)]
14. Ghosh, T.; Elvidge, C.D.; Sutton, P.C.; Baugh, K.E.; Ziskin, D.; Tuttle, B.T. Creating a global grid of distributed fossil fuel CO₂ emissions from nighttime satellite imagery. *Energies* **2010**, *3*, 1895–1913. [[CrossRef](#)]
15. Shi, K.F.; Chen, Y.; Yu, B.L.; Xu, T.B.; Yang, C.S.; Li, L.Y.; Huang, C.; Chen, Z.Q.; Liu, R.; Wu, J.P. Detecting spatiotemporal dynamics of global electric power consumption using DMSP-OLS nighttime stable light data. *Appl. Energy* **2016**, *184*, 450–463. [[CrossRef](#)]
16. Shi, K.; Yu, B.; Hu, Y.; Huang, C.; Chen, Y.; Huang, Y.; Chen, Z.; Wu, J. Modeling and mapping total freight traffic in China using NPP-VIIRS nighttime light composite data. *GISci. Remote Sens.* **2015**, *52*, 274–289. [[CrossRef](#)]
17. He, C.Y.; Shi, P.J.; Li, J.G.; Chen, J.; Pan, Y.Z.; Li, J.; Zhuo, L.; Toshiaki, I. Restoring urbanization process in China in the 1990s by using non-radiance calibrated DMSP/OLS nighttime light imagery and statistical data. *Chin. Sci. Bull.* **2006**, *51*, 1614–1620. [[CrossRef](#)]
18. Yu, B.L.; Shu, S.; Liu, H.X.; Song, W.; Wu, J.P.; Wang, L.; Chen, Z.Q. Object-based spatial cluster analysis of urban landscape pattern using nighttime light satellite images: A case study of China. *Int. J. Geogr. Inf. Sci.* **2014**, *28*, 2328–2355. [[CrossRef](#)]
19. Xiao, P.; Wang, X.; Feng, X.; Zhang, X.; Yang, Y. Detecting China’s urban expansion over the past three decades using nighttime light data. *IEEE J. Sel. Top. Appl. Earth Obs. Remote Sens.* **2014**, *7*, 4095–4106. [[CrossRef](#)]
20. Ma, T.; Yin, Z.; Li, B.; Zhou, C.; Haynie, S. Quantitative estimation of the velocity of urbanization in China using nighttime luminosity data. *Remote Sens.* **2016**, *8*, 94. [[CrossRef](#)]
21. Zhou, Y.Y.; Smith, S.J.; Elvidge, C.D.; Zhao, K.G.; Thomson, A.; Imhoff, M. A cluster-based method to map urban area from DMSP/OLS nightlights. *Remote Sens. Environ.* **2014**, *147*, 173–185. [[CrossRef](#)]
22. Elvidge, C.D.; Ziskin, D.; Baugh, K.E.; Tuttle, B.T.; Ghosh, T.; Pack, D.W.; Erwin, E.H.; Zhizhin, M. A fifteen year record of global natural gas flaring derived from satellite data. *Energies* **2009**, *2*, 595–622. [[CrossRef](#)]

23. Zhang, X.; Scheving, B.; Shoghli, B.; Zygarlicke, C.; Wocken, C. Quantifying gas flaring CH₄ consumption using VIIRS. *Remote Sens.* **2015**, *7*, 9529–9541. [[CrossRef](#)]
24. Gaston, K.J.; Duffy, J.P.; Bennie, J. Quantifying the erosion of natural darkness in the global protected area system. *Conserv. Biol.* **2015**, *29*, 1132–1141. [[CrossRef](#)] [[PubMed](#)]
25. Kyba, C.C.M.; Ruhtz, T.; Fischer, J.; Hoelker, F. Lunar skylight polarization signal polluted by urban lighting. *J. Geophys. Res. Atmos.* **2011**, *116*. [[CrossRef](#)]
26. Bennie, J.; Duffy, J.P.; Davies, T.W.; Correa-Cano, M.E.; Gaston, K.J. Global trends in exposure to light pollution in natural terrestrial ecosystems. *Remote Sens.* **2015**, *7*, 2715–2730. [[CrossRef](#)]
27. Jiang, W.; He, G.J.; Long, T.F.; Wang, C.; Ni, Y.; Ma, R.Q. Assessing light pollution in China based on nighttime light imagery. *Remote Sens.* **2017**, *9*, 135. [[CrossRef](#)]
28. Li, X.; Chen, F.; Chen, X. Satellite-observed nighttime light variation as evidence for global armed conflicts. *IEEE J. Sel. Top. Appl. Earth Obs. Remote Sens.* **2013**, *6*, 2302–2315. [[CrossRef](#)]
29. De Souza, C.R.; Zullo, J.; Elvidge, C. Brazil's 2001 energy crisis monitored from space. *Int. J. Remote Sens.* **2004**, *25*, 2475–2482.
30. Li, X.; Li, D. Can nighttime light images play a role in evaluating the Syrian crisis? *Int. J. Remote Sens.* **2014**, *35*, 6648–6661. [[CrossRef](#)]
31. Li, X.; Li, D.; Xu, H.; Wu, C. Intercalibration between DMSP/OLS and VIIRS nighttime light images to evaluate city light dynamics of Syria's major human settlement during Syrian civil war. *Int. J. Remote Sens.* **2017**, *38*, 1–18. [[CrossRef](#)]
32. Witmer, F.D.W.; O'Loughlin, J. Detecting the effects of wars in the caucasus regions of Russia and Georgia using radiometrically normalized DMSP-OLS nighttime lights imagery. *GISci. Remote Sens.* **2011**, *48*, 478–500. [[CrossRef](#)]
33. Coscieme, L.; Sutton, P.C.; Anderson, S.; Liu, Q.; Elvidge, C.D. Dark times: Nighttime satellite imagery as a detector of regional disparity and the geography of conflict. *GISci. Remote Sens.* **2017**, *54*, 118–139. [[CrossRef](#)]
34. Shi, K.F.; Yu, B.L.; Huang, Y.X.; Hu, Y.J.; Yin, B.; Chen, Z.Q.; Chen, L.J.; Wu, J.P. Evaluating the ability of NPP-VIIRS nighttime light data to estimate the gross domestic product and the electric power consumption of China at multiple scales: A comparison with DMSP-OLS data. *Remote Sens.* **2014**, *6*, 1705–1724. [[CrossRef](#)]
35. Li, X.; Xu, H.M.; Chen, X.L.; Li, C. Potential of NPP-VIIRS nighttime light imagery for modeling the regional economy of China. *Remote Sens.* **2013**, *5*, 3057–3081. [[CrossRef](#)]
36. Li, X.; Chen, X.L.; Zhao, Y.S.; Xu, J.; Chen, F.R.; Li, H. Automatic intercalibration of nighttime light imagery using robust regression. *Remote Sens. Lett.* **2013**, *4*, 46–55. [[CrossRef](#)]
37. Shi, K.F.; Huang, C.; Yu, B.L.; Yin, B.; Huang, Y.X.; Wu, J.P. Evaluation of NPP-VIIRS nighttime light composite data for extracting built-up urban areas. *Remote Sens. Lett.* **2014**, *5*, 358–366. [[CrossRef](#)]
38. Yu, B.; Shi, K.; Hu, Y.; Huang, C.; Chen, Z.; Wu, J. Poverty evaluation using NPP-VIIRS nighttime light composite data at the county level in China. *IEEE J. Sel. Top. Appl. Earth Obs. Remote Sens.* **2015**, *8*, 1217–1229. [[CrossRef](#)]
39. Yemeni Crisis (2011–Present). Available online: [https://en.wikipedia.org/wiki/Yemeni_Crisis_\(2011-present\)](https://en.wikipedia.org/wiki/Yemeni_Crisis_(2011-present)) (accessed on 29 August 2016).
40. Yemen Profile—Timeline. Available online: <http://www.bbc.com/news/world-middle-east-14704951> (accessed on 19 June 2017).
41. Version 1 VIIRS Day/Night Band Nighttime Lights. Available online: https://ngdc.noaa.gov/eog/viirs/download_dnb_composites.html (accessed on 18 June 2017).
42. Version 4 DMSP-OLS Nighttime Lights Time Series. Available online: <https://ngdc.noaa.gov/eog/dmsp/downloadV4composites.html> (accessed on 16 June 2017).
43. Gadm Database of Global Administrative Areas. Available online: <http://www.gadm.org/> (accessed on 29 August 2016).
44. Zhao, N.Z.; Samson, E.L. Estimation of virtual water contained in international trade products using nighttime imagery. *Int. J. Appl. Earth Obs. Geoinf.* **2012**, *18*, 243–250. [[CrossRef](#)]
45. Elvidge, C.D.; Zhizhin, M.; Baugh, K.; Hsu, F.C.; Ghosh, T. Methods for global survey of natural gas flaring from visible infrared imaging radiometer suite data. *Energies* **2016**, *9*, 14. [[CrossRef](#)]
46. How Much Oil Is Daesh Producing? Evidence From Remote Sensing. Available online: <https://www.aeaweb.org/conference/2017/preliminary/paper/Drey9fyy> (accessed on 18 June 2017).

47. Viirs Nightfire. Available online: https://ngdc.noaa.gov/eog/viirs/download_viirs_fire.html (accessed on 29 August 2016).
48. Ma, T.; Zhou, C.H.; Pei, T.; Haynie, S.; Fan, J.F. Responses of Suomi-NPP VIIRS-derived nighttime lights to socioeconomic activity in China's cities. *Remote Sens. Lett.* **2014**, *5*, 165–174. [[CrossRef](#)]
49. Jiang, W.G.; Yuan, L.H.; Wang, W.J.; Cao, R.; Zhang, Y.F.; Shen, W.M. Spatio-temporal analysis of vegetation variation in the Yellow River basin. *Ecol. Indic.* **2015**, *51*, 117–126. [[CrossRef](#)]
50. Tian, Y.C.; Bai, X.Y.; Wang, S.J.; Qin, L.Y.; Li, Y. Spatial-temporal changes of vegetation cover in Guizhou Province, Southern China. *Chin. Geogr. Sci.* **2017**, *27*, 25–38. [[CrossRef](#)]
51. Munir, S. Analysing temporal trends in the ratios of PM2.5/PM10 in the UK. *Aerosol Air Qual. Res.* **2017**, *17*, 34–48. [[CrossRef](#)]
52. Cao, R.; Jiang, W.G.; Yuan, L.H.; Wang, W.J.; Lv, Z.L.; Chen, Z. Inter-annual variations in vegetation and their response to climatic factors in the upper catchments of the Yellow River from 2000 to 2010. *J. Geogr. Sci.* **2014**, *24*, 963–979. [[CrossRef](#)]
53. Narayanan, P.; Sarkar, S.; Basistha, A.; Sachdeva, K. Trend analysis and forecast of pre-monsoon rainfall over India. *Weather* **2016**, *71*, 94–99. [[CrossRef](#)]
54. Zhuo, L.; Ichinose, T.; Zheng, J.; Chen, J.; Shi, P.J.; Li, X. Modelling the population density of China at the pixel level based on DMSP/OLS non-radiance-calibrated nighttime light images. *Int. J. Remote Sens.* **2009**, *30*, 1003–1018. [[CrossRef](#)]
55. Li, X.; Ge, L.L.; Chen, X.L. Detecting Zimbabwe's decadal economic decline using nighttime light imagery. *Remote Sens.* **2013**, *5*, 4551–4570. [[CrossRef](#)]
56. Levin, N. The impact of seasonal changes on observed nighttime brightness from 2014 to 2015 monthly VIIRS DNB composites. *Remote Sens. Environ.* **2017**, *193*, 150–164. [[CrossRef](#)]
57. Yemen 2017 Humanitarian Response Plan. Available online: <http://www.unocha.org/yemen> (accessed on 2 May 2017).
58. Saudi Arabia Launches Air Strikes in Yemen. Available online: <http://www.bbc.com/news/world-us-canada-32061632> (accessed on 18 June 2017).
59. U.S. Fingerprints on Attacks Obliterating Yemen's Economy. Available online: https://www.nytimes.com/2016/11/14/world/middleeast/yemen-saudi-bombing-houthis-hunger.html?_r=0 (accessed on 19 June 2017).
60. Yemen Conflict: Twin Suicide Bombings Hit Aden Base. Available online: <http://www.bbc.com/news/world-middle-east-36722447> (accessed on 19 June 2017).
61. Saudi Coalition Bombs Yemen Water Bottling Plant, Killing Dozens of Civilians. Available online: <https://www.commondreams.org/news/2015/08/31/saudi-coalition-bombs-yemen-water-bottling-plant-killing-dozens-civilians> (accessed on 19 June 2017).
62. Yemen Crude Oil Production. Available online: <http://www.tradingeconomics.com/yemen/crude-oil-production> (accessed on 2 May 2017).
63. Monitoring the Syrian Humanitarian Crisis with the JRC's Global Human Settlement Layer and Nighttime Satellite Data. Available online: http://publications.jrc.ec.europa.eu/repository/bitstream/JRC101733/syria_ghsl-template%20jrc%20technical%20reports-online.pdf (accessed on 2 May 2017).
64. Yemen Enforces Curfew in Sanaa amid Clashes with Shiite Rebels. Available online: http://www.thestar.com/news/world/2014/09/20/yemen_enforces_curfew_in_sanaa_amid_clashes_with_shiite_rebels.html (accessed on 19 June 2017).
65. Yemen Declares Nighttime Curfew in Port City of Aden. Available online: <http://wtop.com/world/2016/01/yemen-declares-nighttime-curfew-in-port-city-of-aden/> (accessed on 2 May 2017).
66. Visible Light at Night over Yemen as of 21 July 2015. Available online: http://www.unitar.org/unosat/node/44/2243?utm_source=unosat-unitar&utm_medium=rss&utm_campaign=maps (accessed on 2 May 2017).

